

ESTIMATION OF THE TOTAL OZONE AND NITROGEN DIOXIDE CONTENT FROM THE DATA ON THE SPECTRAL SKY BRIGHTNESS IN THE ZENITH

S.I. Dolgii, V.V. Zuev, V.N. Marichev, A.A. Mitsel',
I.V. Ptashnik, and V.P. Sorokin

*Institute of Atmospheric Optics,
Siberian Branch of the Russian Academy of Sciences, Tomsk
Received July 17, 1995*

A method for estimating the total O₃ and NO₂ content (TC) from measurements of the spectral sky brightness in the zenith is briefly described. Possible errors in reconstructing the TC using two- and four-wavelength differential absorption methods based on the single-scattering model have been thoroughly accounted. The idea of scanning over the spectrum of pairs of wavelengths used for data processing has been realized that allows us to perform statistically vivid reconstruction of the TC of gases under study. Results of numerical calculation of errors in the TC reconstruction have been presented for the case of processing of real signals recorded in the 280–450 nm wavelength range in the daytime over Tomsk. The mean values of relative errors in the TC reconstruction are about 5–7% for ozone and 40–76% for nitrogen dioxide.

INTRODUCTION

The problem of atmospheric ozone has more than semi-centennial history.¹⁰ It goes back to 1920s, when in 1923 the warm layer in the upper atmosphere was discovered. As a result of research carried out over the elapsed period, it was revealed that the ozone, in spite of its low content in the atmosphere, plays a very important role in radiative and physical-chemical processes as well as in biological life on the Earth. In this connection, the atmospheric ozone constantly attracts the attention of specialists in atmospheric monitoring by optical methods.

Along with investigations of the total ozone content in the atmosphere, rather important is the study of those gaseous constituents that take part in photochemical cycles of ozone generation and destruction, in particular, NO₂.

In this paper we describe briefly the equipment intended to measure the spectral brightness of the atmosphere in the 280–1200-nm wavelength range as well as methods for data processing and results of estimation of the O₃ and NO₂ total content in the daytime over Tomsk.

There are a great number of works published in our country and abroad, that are devoted to the problems of estimation of the total content (TC) of atmospheric gases by passive methods. We mention here only some of them.^{1–30} The majority of these works, however, deal with problems of sensing by the direct solar radiation. And although

measurements in the sky zenith are, as known,^{14,16,17} about half the total ozone content (TOC) measurements, methods for such measurements are less well developed.^{1,4,9,12,14,16–18,24,27,30} This is especially valid as among these works only four^{4,9,24,30} study the possibility of direct processing of the zenith observation, i.e., without ozone nomograms obtained from the data of solar observations. The TOC is conventionally estimated from measurements in the sky zenith referred to the measurements against the sun with the use of the so-called zenith graduation coefficient,^{3,12,16,17} which is usually found empirically (or more rarely from calculations for atmospheric models²⁷).

Thus, the results of reconstruction of the TC of gases from the measurements in the zenith turn out to be referred to the measurements against the sun. For this reason, the main theoretical studies are conducted by the transmission method. Advantages and disadvantages of such an approach are obvious. An expression for calculating the direct radiation signals has a simpler (and, correspondingly, easier understood) analytical form than that for signals of scattered radiation. However, to refer the zenith observations to the direct ones, i.e., to construct the zenith graduation coefficient, rather long periodical calibration of a device is required.

In Ref. 4 the idea was put forward of the possibility to construct the zenith ozone nomograms without their reference to measurements against the sun based solely on calculation for the model of single

scattering of light in the atmosphere. This idea was based on close agreement between the empirical and calculated values of the zenith graduation coefficient. Developing this idea, we now make an attempt to study in greater detail the contribution of different factors to the error in the O₃ and NO₂ total content estimation by the above method from measurements of the sky brightness with a specific device.

1. INSTRUMENTATION AND PROCEDURE FOR MEASURING THE SPECTRAL SKY BRIGHTNESS

The block diagram of a spectrophotometer is shown in Fig. 1. The radiation from an atmospheric column is directed with the plane mirror 1 toward the reflecting telescope 2 with a diameter of 30 cm and a focal length of 2 m. The optical axis and the focal plane of the telescope are coincident with the optical axis and the input slit of the MDR-23 monochromator 3 being part of the KSVU-23 measuring complex 4. The spectrum is recorded in two wavelength ranges: 280–350 and 400–500 nm. A signal is recorded by the FEU-100 (5) or FEU-62 (6) photomultiplier depending on the spectral range. The set of changeable filters 7 in MDR-23 serves to eliminate higher-order spectra. The spectral resolution was 0.1 nm for 280–350 nm range and 0.4 nm for 400–500 nm range. The time needed to record a single spectrum with a 0.1-nm step was about 1 min. The linear angle of observations was no more than 7.5·10⁻³ rad.

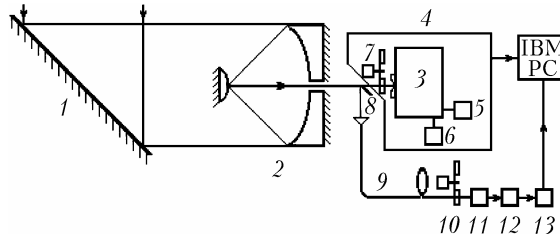


FIG. 1. Block diagram of the spectrophotometer.

To eliminate the effect of signal fluctuations under conditions of broken clouds on the spectral dependence to be recorded, a signal from an operating channel was normalized to a signal from a reference channel that recorded the radiation at a fixed wavelength from the chosen range. The reference channel comprises the mirror 8, which deflects a portion of radiation toward the input of the optical guide 9 through which the radiation passes to the FEU-84 photomultiplier 11. The set of changeable filters 10 serves to select out the spectral ranges in which the reference signal is recorded. A signal from the photomultiplier 11 is fed to the sharpener amplifier 12 and then to the 12-bit ADC 13. The data from the operating and reference channels are then input into an IBM PC for their normalization and further processing. The measurements were conducted during the day with recording of time counts from which the solar elevation angle was determined. Some typical brightness spectra recorded in the 280–705 nm range are shown in Fig. 2.

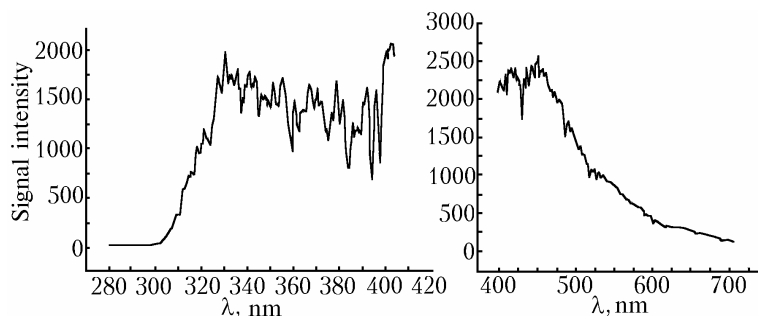


FIG. 2. Brightness spectra recorded for the 280–405 and 400–705 nm wavelength ranges on June 24, 1994.

2. METHODS FOR INTERPRETING THE SPECTRAL SKY BRIGHTNESS MEASUREMENTS

The well-known solution of the radiative transfer equation in the single-scattering approximation³¹ provided the mathematical basis for methods of data interpretation. In this approximation the expression for a signal at the receiver output (for a ground-based device with sighting in the zenith) at the wavelength λ has the form

$$J(\lambda) = S_0(\lambda) C(\lambda) \int_{\Delta\lambda} d\lambda' h(\lambda - \lambda') \int_0^H d(z', \theta, z) \times$$

$$\times \exp \left[- \int_0^z \alpha_{\Sigma}(\lambda', z') dz' - \int_z^H B(z, z', \theta) \alpha_{\Sigma}(\lambda', z') dz' \right] dz, \tag{1}$$

$$\alpha_{\Sigma}(\lambda, z) = k_g(\lambda, z) \rho_g(z) \alpha_a(\lambda, z) + \alpha_m(\lambda, z) + \sum_{i \neq g} k_i(\lambda, z) \rho_i(z),$$

$$d(\lambda, \theta, z) = \alpha'_a(\lambda, z) g_a(\theta) + \alpha_m(\lambda, z) g_m(\theta),$$

$$B(z, z', \theta) = \frac{1}{\sqrt{1 - \left(\frac{R+z}{R+z'} \frac{n(z)}{n(z')} \sin\theta \right)^2}},$$

where $S_0(\lambda)$ is the solar constant; $C(\lambda)$ is the instrumental constant which accounts for the receiving field of view, receiving aperture, optics transmission, receiver's quantum efficiency, and other parameters; θ is the solar zenith angle; $d(\lambda, \theta, z)$ is the total coefficient of aerosol and molecular scattering at an angle θ to the initial propagation direction at an altitude z above the sea level; $k_g(\lambda, z)$ and $k_i(\lambda, z)$ are the vertical profiles of the absorption coefficients of the gas under study and the i th interfering gaseous constituent; H is the effective height of the atmosphere; $\rho_g(z)$ and $\rho_i(z)$ are the vertical profiles of the density of the gas under study and interfering (i.e., the other) gases; $\alpha'_a(\lambda, z)$ and $\alpha'_m(\lambda, z)$ are the profiles of the aerosol and molecular light scattering coefficients; $g_a(\theta)$ and $g_m(\theta)$ are the corresponding light scattering phase functions; $\alpha_a(\lambda, z)$ is the aerosol extinction coefficient; R is the Earth's radius; and, $h(\lambda-\lambda')$ is the instrumental function of the device.

Below we assume that in the interval $\Delta\lambda$ (0.1 nm for ozone and 0.4 nm for NO_2) the optical characteristics can be considered constant.⁶ Therefore, we further ignore the effect of the instrumental function on the results of data interpretation.

Having multiplied the integrand in Eq. (1) by the factor

$$\exp \left[- \int_z^H \alpha_\Sigma(\lambda', z') dz' + \int_z^H \alpha_\Sigma(\lambda', z') dz' \right]$$

and having collected terms, we obtain the expression analogous to that derived in Ref. 4

$$J(\lambda) = S_0(\lambda) C(\lambda) \exp \left[- \int_z^H \alpha_\Sigma(\lambda, z) dz \right] IS(\lambda, \theta), \tag{2}$$

$$IS(\lambda, \theta) = \int_0^H d(\lambda, \theta, z) \times \exp \left\{ \int_z^H \alpha_\Sigma(\lambda, z') [1 - B(z, z', \theta)] dz' \right\} dz.$$

Then, denoting the TC of the gas under study in the

$$\text{atmospheric column by } X = \int_0^H \rho_g(z) dz, \text{ assuming, as is}$$

commonly accepted in ozonometry, k_g to be altitude-independent, i.e., replacing it by the mean effective parameter

$$k_g(\lambda, z) = k_g(\lambda) = \frac{\int k_g(\lambda, z) \rho_g(z) dz}{\int \rho_g(z) dz},$$

and taking the logarithm of Eq. (2), we obtain

$$X = \frac{1}{k_g(\lambda)} \left\{ \ln \frac{S_0(\lambda) C(\lambda)}{J(\lambda)} - [\tau_a(\lambda) + \tau_m(\lambda) + \tau_f(\lambda)] + \ln[IS(\lambda, \theta)] \right\}. \tag{3}$$

Here,

$$\tau_a(\lambda) = \int_0^H \alpha_a(\lambda, z) dz, \quad \tau_m(\lambda) = \int_0^H \alpha_m(\lambda, z) dz, \\ \tau_f(\lambda) = \int_0^H \sum_{i \neq g} [k_i(\lambda, z) \rho_i(z)] dz$$

are the vertical atmospheric optical depths of the aerosol extinction, molecular scattering, and absorption by interfering gaseous constituents, respectively.

In such a way the TC can be reconstructed from the measurements of the radiation scattered in the zenith using the parameters k_g and S_0 available from the literature and the model representations of α_a , α_m , α_f , g_a , and g_m with the known errors. In this connection, the goal of our work is to estimate the mean errors in determining X introduced by the deviation of the model parameters from their true values.

It should be noted that since Eq. (3) is not the rigorous solution for X (X enters into IS), the model information about the profile of the gas under study, $\rho_g(z)$, is also needed. In this case, X is found by the method of successive iterations as $X_{i+1} = F(X_i)$ (F is the right-hand side of Eq. (3)) until $|X_{i+1} - X_i|$ becomes smaller than some preset value.

To decrease the effect of slightly selective components (aerosol and molecular scattering) and variability of the solar constant upon the result of the TC estimation, usually used in practice are two- and four-wavelength methods. Let us consider them in more detail.

1) *Two-wavelength method*

Using Eq. (3) for two wavelengths, we obtain

$$X = \frac{1}{\Delta k_g} \left\{ \ln \frac{S_0^{1,2} C^{1,2}}{J^{1,2}} - [\Delta\tau_a + \Delta\tau_m + \Delta\tau_f] + \ln[IS^{1,2}] \right\}, \tag{4}$$

where superscript 1,2 means the ratio of the corresponding parameters at λ_1 and λ_2 wavelengths [for example, $J^{1,2} = J(\lambda_1)/J(\lambda_2)$], $\Delta\tau = \tau(\lambda_1) - \tau(\lambda_2)$, and $\Delta k_g = k_g(\lambda_1) - k_g(\lambda_2)$.

2) *Four-wavelength method*

When the spectral dependence of the optical depth of the gas under study is nonlinear against the background of slightly selective extinction due to interfering constituents, the four-wavelength method will be efficient, because it allows one to decrease the aerosol effect to a greater extent than the two-wavelength method.^{23,26} This method is implemented, for example, in the Dobson device.¹³ In this case, the expression for X has the form similar to Eq. (4)

$$X = \frac{1}{\tilde{\Delta}k_g} \left\{ \ln \left[\frac{S_0^{1,2} C^{1,2} J^{3,4}}{S_0^{3,4} C^{3,4} J^{1,2}} \right] - [\tilde{\Delta}\tau_a + \tilde{\Delta}\tau_m + \tilde{\Delta}\tau_f] + \ln \frac{IS^{1,2}}{IS^{3,4}} \right\}, \quad (5)$$

where the symbol $\tilde{\Delta}$ is introduced for the second differences of the corresponding parameters.

3. ERROR IN THE TC ESTIMATION

To estimate the possible errors in determining TC of the gases under study from Eqs. (4) and (5), we used the well-known method for determining the errors of indirect measurements,⁴³⁻⁴⁵ since in our case the error in determining the sought-after parameter depends on the errors in determining a number of the other measurable and preset parameters. The total relative error in X estimation from measurements at two (or four) wavelengths was calculated by the formula

$$\delta X_{\Sigma} = \sqrt{\sum_{i=1}^n (\delta X_i)^2}, \quad \delta X_i = \left(\frac{\Delta X_i}{X_i} \right), \quad (6)$$

where δX_i is the relative error in TC determination due to error (Δy_i) in determination of the i th argument of the function $X(y_1, y_2, \dots, y_i, \dots, y_n)$,

$$\Delta X_i = X(y_1, y_2, \dots, y_i + \Delta y_i, \dots, y_n) - X(y_1, y_2, \dots, y_i, \dots, y_n), \quad (6a)$$

n is the number of arguments whose errors are taken into consideration. Usually, the formula similar to Eq. (6) is used for random Δy_i (Refs. 13 and 19). However, in Refs. 45 and 46, for example, the possibility and the correctness were rightly justified of using this formula for systematic errors as well. By virtue of the fact that the sign of Δy_i can be random for different i , the total error found in such a way will characterize the standard deviation of the sought-after parameter from its true value rather than its maximum deviation (as in the case of direct summation).

The errors in the arguments y_i were mainly borrowed from the literature. Below we list the absolute, Δy_i , and relative, $\delta y_i = \Delta y_i / y_i$, errors which were taken into our consideration.

1) The relative error in assignment of the absorption coefficient of the gas under study δk_g was taken to be 3% for the entire wavelength range for both ozone and NO₂ (see Refs. 1, 10, 13, 19, 26, 38, and 41).

2) The relative error in measuring the ratio of signals at two wavelengths (the signal error) $\delta J^{1,2}$. For ozone, due to wide variability of SNR in the 295–330 nm range, $\delta J^{1,2}$ was estimated for every pair of wavelengths based on the rms noise level. In the region of the minimum total error δX_{Σ} for ozone ($\lambda \approx 304$ – 305 nm), the signal error usually was 2–3%. For NO₂ the signal error was taken 1% over the entire spectral

range in accordance with its estimates accepted in the literature.^{15,19}

3) The relative error in assigning the ratio of the solar constants at two wavelengths $\delta S_0^{1,2}$ was taken 3% when estimating the ozone TC and 1% for NO₂ (Refs. 15, 19, 39, and 40), though Gushchin,¹⁹ for example, considered these values to be underestimated.

4) The absolute error in determining the solar zenith angle $\Delta\theta$ was taken 20' for our measurement conditions.

5) The relative error in assigning the vertical optical depth of molecular scattering $\delta\tau_m$ was taken 5%. It can be considered even as overestimated value.^{13,15,19}

6) The relative error in assigning the vertical aerosol optical depth $\delta\tau_a$ with regard for wide variability of the atmospheric aerosol, was taken 200%. Taking into account the fact that in the visible and near-UV spectral ranges the aerosol optical depth of the cloudless atmosphere varies within 0.02–0.4 (Ref. 19) (to base 10) and that in our aerosol model it is 0.15 for $\lambda = 369$ nm (Refs. 22 and 47), we can say that with the given $\delta\tau_a$ the aerosol fluctuations, on average, are well covered by the range of variability mentioned above.

7) The absolute wavelength referencing error $\Delta\lambda$. The contribution of this error to the error in the TC determination from measurements against the sun was estimated in sufficient detail, for example, in Ref. 21. In our measurements $\Delta\lambda$ was taken 0.05 nm.

8) The relative error in assigning the vertical optical depth of interfering gases $\delta\tau_f$. When estimating TC of NO₂, the ozone was considered as an interfering gas and $\delta\tau_{O_3}$ was taken 50%. With the mean total ozone content (TOC) being equal to about 330 Dobson units, this value also covers the range of possible TOC variations in the atmosphere.^{5,48,49} When estimating TOC, SO₂ and NO₂ were considered as interfering gases, and $\delta\tau_{NO_2}$ and $\delta\tau_{SO_2}$, with regard for wide variability of TC of these gases in the atmosphere, were taken 1000% each (Refs. 13, 15, and 42).

4. MODELS USED TO ESTIMATE TC OF GASES

Below we list the models used to estimate TC of gases and errors in TC reconstruction.

a) The vertical profiles of gases were taken from the meteorological model for the mid-latitudes in summer.³² The model TC in this case was varied by multiplying $\rho_i(z)$ by the altitude-independent multiplier.

b) The aerosol model for $\alpha_a(\lambda, z)$ was borrowed from Ref. 33 (background model) and multiplied by 2.5 for all altitudes in order to make the aerosol optical depth equal to 0.15 (to base 10) that corresponds to many-year average values of the atmospheric aerosol density obtained at the meteorological stations of the former USSR for $\lambda = 369$ nm (Refs. 22 and 47). If the well-known Angström formula $\tau_a(\lambda) = C\lambda^{-b}$ is used for aerosol optical depth approximation, then in our model

$b = 0.82$ and $C = 0.0656$ (0.151 with natural logarithmic base).

c) The coefficient of molecular scattering was calculated by the formula

$$\alpha_m(\lambda, z) = \frac{4.85 \cdot 10^4 P(z)}{\lambda^4 T(z)} \left(77.6 + \frac{584000}{\lambda^2} \right)^2, [\text{km}^{-1}],$$

where $P(z)$ is the air pressure [mbar], λ is the wavelength [nm], and $T(z)$ is the temperature [K].

d) The aerosol and molecular scattering phase functions were calculated by the formulas

$$g_m(\theta) = \frac{3}{16\pi} (1 + \cos^2\theta),$$

$$g_a(\theta) = \frac{36.6 \cdot 10^{-3}}{(1.49 - 1.4 \cos\theta)^{3/2}}, [\text{sr}^{-1}].$$

The latter formula is the approximation of $g_a(\theta)$ by the Henyey-Greenstein formula³¹ for the model of Ref. 33. The coefficient of aerosol light scattering $\alpha'_a(\lambda, z)$ can be taken, with good accuracy, equal to the coefficient of aerosol extinction $\alpha_a(\lambda, z)$ within the spectral range we use.

e) The interfering gases when estimating TOC, SO_2 and NO_2 , were taken into consideration based on the data on their absorption coefficients^{34,35,41} and concentration.^{36,37} The ozone absorption cross sections were borrowed from Ref. 38.

f) The spectral dependence $S_0(\lambda)$ was borrowed from Ref. 40. Our attempt to use the solar constant measured by Thekaekara³⁹ yielded the least reliable and stable results. And in this case, in the 300–350 nm region the extrema of the Thekaekara function $S_0(\lambda)$ were shifted with respect to those obtained by processing of signals being recorded. This shift reached 1 nm in the 300–315 nm region. The similar discrepancy was also observed in Ref. 28.

5. RESULTS OF PROCESSING OF ATMOSPHERIC SPECTRAL BRIGHTNESS SIGNALS

Figure 2 shows the sky spectral brightness measured in an experimental run on June 24, 1994. To estimate the ozone and NO_2 total content, we used the spectral ranges 300–330 and 430–450 nm, respectively. To process the data using the procedures described above, the idea was implemented of scanning over the spectrum of differential pairs of wavelengths with the same or different steps for “onB and “offB wavelengths. The same procedure was used, for example, in Refs. 23, 28, and 29. The curves of spectral dependence (on λ_{on} , for example) of the reconstructed ozone and NO_2 concentration obtained in such a way represent fluctuating (due to random errors) broken lines with more or less pronounced platform in the region of the minimum reconstruction error (Figs. 3 and 4). The level of this platform and the spread of values about it allow the statistical analysis to be carried out in order to find the sought-after TC of the gas under study.

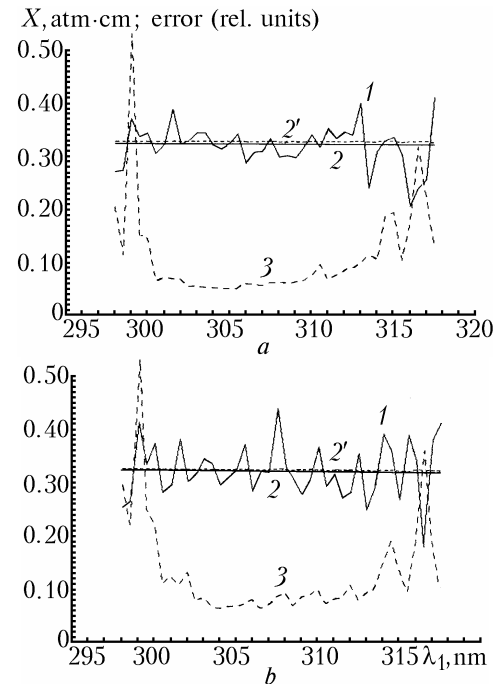


FIG. 3. Results of TOC reconstruction from signals measured at a solar zenith angle of 56.8° on June 24, 1994.

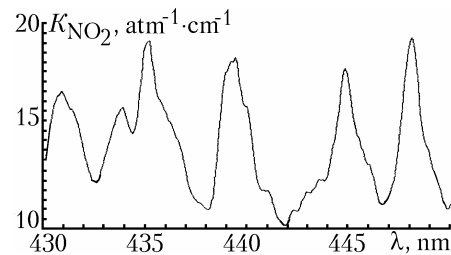


FIG. 4. The NO_2 absorption coefficient⁴¹ under normal conditions ($T = 273$ K) averaged with a 0.4-nm resolution.

The mean value and the rms errors of reconstructed TC were determined by the formulas

$$\bar{X} = \sum_{j=1}^m X(j) P(j), \quad \delta X_{\Sigma}(j) = \sqrt{\sum_{i=1}^n [\delta X_{\Sigma}(j)]^2}, \quad (7)$$

$$\sigma_{\Sigma} = \sqrt{\sum_{i=1}^n \sigma_i^2}, \quad \sigma_i = \sqrt{\sum_{j=1}^m [\delta X_i(j)]^2 P(j)}, \quad (8)$$

where subscripts i and n denote the serial order and the number of arguments of the function $X(y_1, y_2, \dots, y_i, \dots, y_n)$ whose errors are taken into consideration (in our case, $n = 8$, see Section 3), whereas subscripts j and m are for the serial order and the number of pairs (or quadruplets for four-wavelength method) of wavelengths included in processing; $P(j)$ is the normalized weighting function that describes the reliability of $X(j)$ (the TC obtained

by signal processing for the j th pair of wavelengths) and depends on the total reconstruction error for the j th pair, i.e., $P(j) = F(\delta X_{\Sigma}(j))$.

One of the advantages of such an approach is the possibility to select an optimal operating region with minimum $\delta X_{\Sigma}(j)$ depending on specific measurement conditions, which was pointed out, for example, in Ref. 26.

We do not completely agree with the opinion of Luydchik et al.²³ that the contribution of systematic errors (for example, $\delta S_0^{1,2}$ or δk_g) cannot be decreased simply by going to the multiwavelength measurement technique. The point is that these errors, even being systematic from the viewpoint of their invariability for each wavelength, will be quasirandom ones in the multiwavelength technique we use because for different wavelengths their sign varies quasirandomly. This all manifests itself through quasirandom fluctuations (both positive and negative) of TC reconstructed for different pairs of wavelengths about its true (mean) value, which in this case can be found with the accuracy proportional to \sqrt{m} (see, for example, Fig. 3). The possibility of such transformation of systematic errors into quasirandom ones was discussed, for example, in Ref. 44. For such y_i the expression for rms error σ_i , entering into Eq. (8), will have the form

$$\sigma_i = \sqrt{\frac{1}{m} \sum_{j=1}^m [\delta X_i(j)]^2 P(j)}. \quad (9)$$

Let us consider in more detail the results of signal processing to estimate the O₃ and NO₂ total content.

a) Ozone. As an example, Fig. 3 shows the results of processing of signals measured at a solar zenith angle of 56.8° on June 24, 1994. Curve 1 is for the TOC determined by the two-wavelength (*a*) and four-wavelength (*b*) methods of differential absorption. The solid horizontal line 2 is for the TOC obtained by averaging $X(j)$ by Eq. (7). The dashed horizontal line 2' is for the TOC measured with the M-124 ozonometer with an error of 5%. The dashed curve 3 shows the total relative error in the TOC reconstruction for the j th pair of wavelengths $\delta X_{\Sigma}(j)$, [see Eq. (6)], in relative units. The wavelengths in Figs. 3*a* and *b* were changed in such a way: $\lambda_1 = 298.0$ (0.5) and $\lambda_2 = 319.0$ (0.1) nm for the two-wavelength method and $\lambda_1 = 298.0$ (0.5), $\lambda_2 = 319.0$ (0.1), $\lambda_3 = 304.0$ (0.5), and $\lambda_4 = 319.0$ (0.1) nm for the four-wavelength method. Given in parentheses is the step of scanning. It can be seen from Fig. 3 that the spectral range of the most stable results (with minimum fluctuations of the reconstructed TOC) well coincides with the region of the minimum calculated error $\delta X_{\Sigma}(j)$ (-5-7%) and corresponds to 300.5-310 nm for the two-wavelength method. The increase of the error to the left of this region is due to the signal error $\delta J^{1,2}$ (a signal becomes comparable to noise) and the calibration error $\Delta\lambda$. The increase of the error to the right of it is mainly due to the increase of errors $\delta S_0^{1,2}$, δk_g , $\delta\tau_a$, and $\Delta\lambda$.

For the four-wavelength method, the minimum of $\delta X_{\Sigma}(j)$ is somewhat shifted toward longer wavelengths (304.5-313 nm) as compared with the two-wavelength method. This is due to the increasing contribution of the signal error (to the left of 304 nm) and the decreasing contribution of $\delta\tau_a$ and $\Delta\lambda$ to the right of 310 nm.

A contribution of each error to the total one can be evaluated from Tables I and II that give the results of the TC reconstruction shown in Figs. 3*a* and *b*. Listed in these tables are the values of the initial errors (δy_i) of all arguments and the corresponding errors ($\delta X_i(j)$) of the TC reconstruction. Presented at the bottom of the tables are: the gas under study, the solar zenith angle at which the measurement was conducted, the reconstructed TC of the gas under study (and its value measured with the M-124 ozonometer), the model TC of interfering gases, pairs of wavelengths used for processing with the scanning step for each of them. The first column presents the pairs of wavelengths and the second column gives the total error for each pair. Separate components of the total error are tabulated in columns 3-11. The signal error $\delta J^{1,2}$, as was already mentioned, was calculated for ozone for each pair separately. It is presented in parentheses in corresponding column adjacent to $\delta X_{j,1,2}$. For the four-wavelength technique (Table II) we give only the first pairs of wavelengths to save room. At the bottom of both tables the values of σ_i and σ_{Σ} (see Eq. (8)) are presented. In this case, $\sigma_{j,1,2}$ was calculated by Eq. (9) for random errors, whereas the values of σ_{k_g} , $\sigma_{S_0^{1,2}}$, and σ_{λ} were calculated by both Eq. (8) (upper value) and Eq. (9) (lower value in parentheses) on the assumption of their quasirandom character (see comments to Eq. (9)). The value of σ_{Σ} obtained in this case is also presented below in parentheses.

In this connection, it should be noted that the character of $X(j)$ fluctuations shown in Fig. 3 and the intercomparison of measurements made at different times allow us to conclude that these fluctuations are due to the quasirandom alternation of the sign (at different wavelengths) of the errors δk_g , $\delta S_0^{1,2}$, and $\delta\lambda$ rather than the random character of the signal error $\delta J^{1,2}$. This well supports the above assumption.

It is seen from Tables I and II that the main sources of error in the TOC reconstruction by the both methods are:

- 1) error in assigning the ozone absorption coefficient $\delta k_g = 3\%$ resulting in $\sigma_{k_g} \approx 3.7$ and 6% for the two- and four-wavelength methods, respectively;
- 2) error in assigning the aerosol component $\delta\tau_a = 200\%$ resulting in $\sigma_{\tau_a} \approx 4.2$ and 3.6%, respectively;
- 3) wavelength referencing error $\Delta\lambda = 0.05$ nm $\rightarrow \sigma_{\lambda} \approx 3.5$ and 5.3%;
- 4) error in assigning the solar constant $\delta S_0^{1,2} = 2\% \rightarrow \sigma_{S_0^{1,2}} \approx 1.9$ and 2.7%.

However, taking into account the fact that the 1st, 3rd, and 4th errors are likely quasirandom in character for different wavelengths and therefore their contribution can be decreased by averaging over many pairs of wavelengths, most important becomes the error in assigning the aerosol component. However, it also can be decreased not only by more accurate selection of pairs of wavelength in the four-wavelength method, but also by simultaneous processing of signals (using the least-square method,

for example) at many wavelengths, i.e., with the help of the multiwavelength method analogous to that used, for example, in Refs. 2, 11, and 26 for the transmission method. In so doing the case in point is simultaneous processing with regard for correlation between signals at all wavelength in a set rather than processing of a large number of pairs (or quadruplets) of wavelengths. Up to date, we are not aware of such a technique developed for observations of the scattered sky radiation in the zenith.

TABLE I. Results of calculation of the errors in the TOC reconstruction by the two-wavelength method corresponding to Fig. 3a. Gas under study is O_3 , $\theta = 56.8^\circ$, $X_{O_3} = 0.326$ atm-cm (the M-124 ozonometer gives $X_{O_3} = 0.330$ atm-cm), $X_{SO_2} = 0.738 \cdot 10^{-4}$ atm-cm, $X_{NO_2} = 4.000 \cdot 10^{-4}$ atm-cm, $\lambda_1 = 300$ nm (in 0.5-nm step), and $\lambda_2 = 319.4$ nm (in 0.1-nm step).

$\lambda_1 - \lambda_2$, nm	δu_Σ	δk_g	$\delta X_{J1.2}(\delta J^{1.2})$	$\delta S^{1.2}$	$\delta \theta$	$\delta \tau_m$	$\delta \tau_a$	$\delta \lambda$	$\delta \tau_{SO_2}$	$\delta \tau_{NO_2}$
		3%		2%	20'	5%	200%	0.05 nm	1000%	1000%
		δX_{kg}		$\delta X_{S^{1.2}}$, %	δX_θ	δX_{τ_m}	δX_{τ_a}	δu_λ	δX_{SO_2}	δX_{NO_2}
300.0–319.4	14.58	3.24	11.30(53.6)	0.43	0.63	0.18	1.94	8.36	0.04	0.37
300.5–319.5	6.44	3.27	4.72(21.0)	0.46	0.62	0.23	2.30	1.53	0.04	0.47
301.0–319.6	7.13	3.30	3.86(16.0)	0.50	0.64	0.24	2.27	4.36	0.04	0.48
301.5–319.7	6.77	3.33	5.32(20.8)	0.52	0.68	0.22	1.92	1.34	0.03	0.41
302.0–319.8	6.76	3.35	2.79(10.5)	0.56	0.66	0.28	2.39	4.46	0.04	0.50
302.5–319.9	5.37	3.39	2.88(10.1)	0.60	0.67	0.29	2.45	1.38	0.04	0.51
303.0–320.0	5.43	3.45	2.21(7.1)	0.67	0.69	0.32	2.52	2.25	0.04	0.53
303.5–320.1	5.16	3.44	1.71(5.3)	0.70	0.69	0.34	2.59	1.92	0.03	0.55
304.0–320.2	5.09	3.42	1.48(4.6)	0.72	0.69	0.36	2.77	1.69	0.03	0.62
304.5–320.3	4.97	3.42	1.28(3.7)	0.78	0.69	0.40	2.97	0.87	0.03	0.68
305.0–320.4	4.97	3.44	1.05(2.9)	0.87	0.70	0.43	3.08	0.51	0.03	0.70
305.5–320.5	4.97	3.44	1.03(2.6)	0.93	0.71	0.43	3.05	0.65	0.02	0.73
306.0–320.6	5.96	3.42	0.93(2.4)	0.96	0.70	0.52	3.65	2.67	0.02	0.89
306.5–320.7	5.89	3.41	0.90(2.3)	0.98	0.71	0.48	3.39	2.92	0.01	0.79
307.0–320.8	5.51	3.43	0.74(1.7)	1.11	0.72	0.53	3.67	1.37	0.00	0.80
307.5–320.9	6.21	3.46	0.71(1.5)	1.26	0.73	0.56	3.72	3.04	0.01	0.81
308.0–321.0	6.33	3.42	0.67(1.4)	1.26	0.72	0.60	4.04	2.88	0.05	0.93
308.5–321.1	5.96	3.46	0.69(1.4)	1.37	0.72	0.63	4.20	1.30	0.35	0.95
309.0–321.2	6.27	3.48	0.70(1.3)	1.44	0.72	0.65	4.35	1.99	0.35	0.81
309.5–321.3	6.56	3.56	0.79(1.3)	1.66	0.74	0.69	4.48	2.26	0.36	0.78
310.0–321.4	7.54	3.62	0.80(1.2)	1.81	0.75	0.68	4.39	4.32	0.34	0.87
310.5–321.5	9.74	3.65	0.71(1.0)	1.91	0.74	0.74	4.80	7.22	0.36	0.97
311.0–321.6	6.77	3.79	0.68(0.9)	2.05	0.75	0.68	4.43	2.31	0.32	0.84
311.5–321.7	7.68	3.91	0.69(0.9)	2.15	0.75	0.73	4.73	3.77	0.32	0.88
312.0–321.8	8.73	4.27	0.85(0.9)	2.68	0.76	0.86	5.41	4.26	0.36	1.05
312.5–321.9	9.14	4.66	0.99(0.9)	3.18	0.77	1.01	6.24	2.97	0.39	1.10
313.0–322.0	10.17	5.08	1.10(0.9)	3.60	0.78	0.93	5.74	5.24	0.34	1.17
313.5–322.1	11.66	4.74	0.97(0.8)	3.28	0.75	1.31	8.32	5.05	0.48	2.09
314.0–322.2	10.58	5.11	1.16(0.8)	3.94	0.77	1.18	7.40	2.79	0.43	2.02
314.5–322.3	19.02	5.92	1.59(0.8)	5.44	0.79	1.49	9.05	14.30	0.54	2.27
315.0–322.4	19.69	5.90	1.62(0.8)	5.58	0.79	1.41	8.63	15.43	0.51	1.90
315.5–322.5	10.62	5.12	1.27(0.8)	4.38	0.77	1.12	7.16	3.02	0.42	1.84
316.0–322.6	17.64	5.96	1.83(0.8)	6.29	0.79	2.26	14.03	3.29	0.84	4.32
316.5–322.7	32.15	6.77	2.29(0.8)	7.95	0.81	2.33	14.32	26.19	0.86	4.68
317.0–322.8	22.64	6.53	2.14(0.7)	7.69	0.80	1.96	12.20	15.51	0.73	3.44
$\sigma(\%)$:	7.00 (4.70)	3.73 (0.94)	0.75	1.93 (0.49)	0.71	0.63	4.18	3.53 (0.90)	0.23	0.96

TABLE II. Results of calculation of the errors in the TOC reconstruction by the four-wavelength method corresponding to Fig. 3b. Presented are only the first pairs of wavelengths. Gas under study is O_3 , $\theta = 56.8^\circ$, $X_{O_3} = 0.329$ atm-cm (the M-124 ozonometer gives $X_{O_3} = 0.330$ atm-cm), $X_{SO_2} = 0.738 \cdot 10^{-4}$ atm-cm, $X_{NO_2} = 4.00 \cdot 10^{-4}$ atm-cm, $\lambda_1 = 300$ nm (in 0.5-nm step), $\lambda_2 = 319.4$ nm (in 0.1-nm step), $\lambda_3 = 306$ nm (in 0.5-nm step), and $\lambda_4 = 319.4$ nm (in 0.1-nm step).

$\lambda_1 - \lambda_2$, nm	δX_Σ	δk_g	$\delta X_{J1,4}$ ($\delta J^{1,2}$)	$\delta S^{1,2}$	$\delta \theta$	$\delta \tau_m$	$\delta \tau_a$	$\delta \lambda$	$\delta \tau_{SO_2}$	$\delta \tau_{NO_2}$
		3%		2%	20'	5%	200%	0.05 nm	1000%	1000%
		δX_{kg}		$\delta X_{S^{1,4}}$, %	δX_θ	δX_{τ_m}	δX_{τ_a}	δX_λ	δX_{SO_2}	δX_{NO_2}
300.0–319.4	22.35	5.93	19.40(53.6)	0.73	0.60	0.01	1.10	9.28	0.06	0.16
300.5–319.5	11.17	6.09	8.51(21.0)	0.83	0.53	0.04	1.62	3.37	0.09	0.30
301.0–319.6	12.65	5.88	6.60(16.0)	0.85	0.57	0.06	1.54	8.85	0.09	0.34
301.5–319.7	10.96	5.63	8.46(20.8)	0.83	0.65	0.06	1.16	3.80	0.07	0.24
302.0–319.8	13.44	5.79	4.59(10.5)	0.91	0.61	0.09	1.58	11.05	0.05	0.21
302.5–319.9	7.93	5.80	4.65(10.1)	0.96	0.63	0.11	1.57	1.91	0.15	0.19
303.0–320.0	8.78	6.18	3.67(7.1)	1.10	0.66	0.14	1.57	4.60	0.15	0.27
303.5–320.1	6.89	5.77	2.71(5.3)	1.10	0.66	0.15	1.62	1.53	0.15	0.30
304.0–320.2	6.51	5.49	2.28(4.6)	1.09	0.65	0.16	1.83	1.41	0.16	0.30
304.5–320.3	7.00	5.67	2.00(3.7)	1.20	0.66	0.19	1.88	2.70	0.16	0.30
305.0–320.4	6.96	6.04	1.72(2.9)	1.40	0.68	0.24	2.04	1.49	0.17	0.37
305.5–320.5	7.44	6.47	1.77(2.6)	1.58	0.70	0.25	1.96	1.81	0.16	0.43
306.0–320.6	8.25	5.67	1.46(2.4)	1.48	0.67	0.29	2.43	4.97	0.19	0.60
306.5–320.7	6.68	5.39	1.34(2.3)	1.45	0.69	0.25	2.11	2.51	0.15	0.56
307.0–320.8	7.30	5.66	1.17(1.7)	1.69	0.70	0.32	2.43	3.20	0.17	0.52
307.5–320.9	8.88	6.98	1.29(1.5)	2.22	0.73	0.34	2.25	4.20	0.16	0.39
308.0–321.0	9.63	5.98	1.11(1.4)	2.00	0.71	0.38	2.72	6.59	0.10	0.55
308.5–321.1	7.18	5.33	1.03(1.4)	1.96	0.71	0.40	2.89	2.94	0.31	0.70
309.0–321.2	8.97	5.41	1.06(1.3)	2.09	0.70	0.47	3.35	5.76	0.34	0.73
309.5–321.3	9.16	7.06	1.45(1.3)	2.93	0.72	0.65	4.14	2.15	0.42	0.70
310.0–321.4	10.43	6.13	1.29(1.2)	2.77	0.74	0.50	3.27	7.06	0.31	0.57
310.5–321.5	7.65	5.59	1.07(1.0)	2.71	0.72	0.61	4.02	1.03	0.35	0.72
311.0–321.6	8.58	5.86	1.02(0.9)	2.91	0.73	0.61	3.98	3.50	0.32	0.81
311.5–321.7	8.88	6.05	1.04(0.9)	3.05	0.72	0.74	4.86	2.33	0.36	1.29
312.0–321.8	11.24	6.45	1.24(0.9)	3.66	0.74	0.88	5.53	5.95	0.39	1.57
312.5–321.9	8.48	5.72	1.17(0.9)	3.51	0.75	0.66	4.23	2.39	0.27	0.84
313.0–322.0	9.85	5.52	1.19(0.9)	3.64	0.74	0.97	6.24	3.19	0.35	1.10
313.5–322.1	10.83	6.38	1.22(0.8)	3.85	0.75	0.87	5.61	5.05	0.32	1.37
314.0–322.2	15.41	8.08	1.65(0.8)	5.24	0.77	0.92	5.62	10.25	0.33	1.91
314.5–322.3	19.64	7.03	1.72(0.8)	5.55	0.78	1.05	6.45	15.98	0.38	1.94
315.0–322.4	14.16	5.52	1.46(0.8)	4.73	0.76	1.17	7.42	9.32	0.43	1.27
315.5–322.5	10.04	4.92	1.17(0.8)	3.79	0.76	0.62	4.15	6.49	0.24	0.73
316.0–322.6	19.62	8.51	2.24(0.8)	7.25	0.80	1.44	8.81	12.98	0.53	2.32
316.5–322.7	36.97	8.61	2.67(0.8)	8.69	0.82	3.25	19.85	27.62	1.20	6.38
317.0–322.8	19.59	7.20	2.12(0.7)	7.08	0.80	1.23	7.72	14.51	0.46	2.13
σ (%):	9.25	5.95	1.06	2.66	0.70	0.53	3.56	5.27	0.25	0.80
	(4.45)	(1.52)		(0.68)				(1.35)		

As seen from Tables I and II, the errors due to uncertainty in the SO_2 and NO_2 content are within 1% with $X_{SO_2} \approx 0.7 \cdot 10^{-4}$ and $X_{NO_2} \approx 4.0 \cdot 10^{-4}$ atm-cm (Ref. 36). It should be noted, however, that for extremely high content of these gases in industrial regions reaching, according to Ref. 42, -0.05 atm-cm, the error in the TOC reconstruction due to neglect of these constituents can reach, as our calculations show, 2.5% ($\lambda_1 < 308$ nm) – 20% ($\lambda_1 > 308$ nm) for SO_2 and 6–10% for NO_2 . This agrees well with the analogous estimates of Ref. 13 for the TOC measurements against the sun using the Dobson spectrophotometer.

In conclusion, it should be noted that preliminary results of processing of signals received in different days (including a few cloudy days) showed that the deviation of the values of TOC reconstructed by our method from those measured with the M-124 meter, on average, is 2–4%. Only one day the difference was about 7%, which also agrees with our estimates of the rms error in the TOC reconstruction. As a rule (it also can be seen from Figs. 3a and b), the real variance of error in the reconstructed TOC values is smaller for the two-wavelength method than for the four-wavelength one.

However, sometimes the systematic bias of the reconstructed TOC values from those measured with the M-124 meter was somewhat greater for the two-wavelength method as compared to the four-wavelength one.

As follows from the results of our calculations presented in Tables I and II, the total error in the TC estimation by the four-wavelength method may be greater or smaller than that by the two-wavelength method. Decreasing the contribution of aerosol (plus), the four-wavelength method increases the contribution of the signal error and the errors δk_g , $\delta S_0^{1,2}$, and $\delta \lambda$, thereby adding the parameters y_i into Eq. (6) (minus). The relation between the total errors σ_Σ for these two methods depends on the degree of compensation for these pluses and minuses in the four-wavelength method and on the degree of quasirandomness of the above-listed errors. We hope that this comment will clear up, even if to some extent, the misunderstanding about the effect of many wavelengths used on the error in the TOC reconstruction discussed in Refs. 19, 20, and 25.

b) NO₂. The most stable results of reconstruction of the NO₂ content were obtained with λ_1 ranging between 438.0 and 441.0 nm. In this case, $\lambda_2 = 441.7$ nm remained unchanged that corresponds to the minimum NO₂ absorption in this spectral range⁴¹ (see Fig. 4).

The results of reconstruction of the NO₂ total content at a solar zenith angle of 89° for July 14, 1995 are shown in Fig. 5. According to Ref. 9 as well as to the estimation formulas derived in Ref. 13, the contribution from multiple scattering to the net radiation from the sky zenith can be neglected for the spectral range near 440 nm at zenith angles up to 93–94°. As in the case of ozone, the platform is observed in the spectral behavior of reconstructed TC of NO₂ (at a level of $4.6 \cdot 10^{-4}$ atm·cm) with minimum error of about 55–60%. More sharp, as compared to ozone, extrema of $\delta X_\Sigma(j)$ engage our attention. They are due to more selective spectral behavior of the NO₂ absorption coefficient in the range under study.

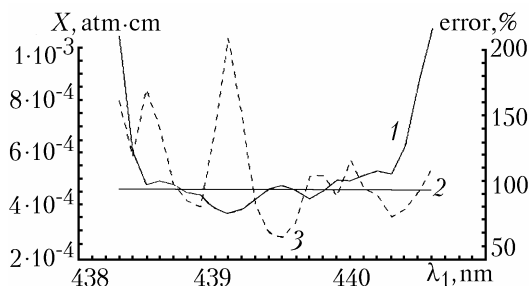


FIG. 5. Results of the NO₂ TC reconstruction from the signals recorded at the solar zenith angle $\theta = 89^\circ$ on July 14, 1995. The wavelengths are $\lambda_1 = 438.0$ in a 0.1-nm step and $\lambda_2 = 441.7$ nm without scanning.

Table III (similarly to Tables I and II) presents the values of the total error in the NO₂ TC reconstruction and its constituents. The signal error $\delta J^{1,2}$ was taken 1% for all wavelengths. It is seen that the main contribution to the total rms error comes from the errors caused by:

- uncertainty in the solar constant, 18–48%;
- uncertainty in the wavelength, 19–50%;
- signal error, 17%;
- neglect of the ozone absorption, 21%.

In this case, the total rms error σ_Σ ranges from 40 to 76% depending on the degree of averaging of the quasirandom errors. The contribution coming from uncertainties in the NO₂ absorption coefficient (4–12%) and in the solar zenith angle (8%) are noticeably smaller.

Let us note that the priority of types of errors and their values, obtained above for ozone and NO₂, well agree with other estimates^{10,11,13,15,19,20,25} for measurements against the sun and zenith. However, further in Table III the abnormally small contribution from the aerosol and the molecular scattering component to the error in the NO₂ TC determination engages our attention.

Thus, according to the estimates of Ref. 7, for example, (and our calculations support that) for the pair of wavelengths 447.7 and 442.0 nm the proportion of the vertical differential optical depths of molecular scattering $\Delta\tau_m$, aerosol in nonturbid atmosphere $\Delta\tau_a$, and NO₂ $\Delta\tau_g$ is 45:12:11. Based on this fact, Garrison et al.⁷ draw a logical conclusion that the selective absorption by aerosol should be taken into account when estimating the NO₂ total content. For the pair of wavelengths we use (439.5 and 441.7 nm) this proportion is 52:12:35, that is, more favorable. Nevertheless, the error in assigning the aerosol component in our calculations should introduce an error into the NO₂ TC determination of the order of 66% ($\approx \delta\tau_g \cdot \Delta\tau_g / \Delta\tau_a$), as follows from the formula for the TC determination when sensing against the sun.^{14,15,19} However, in our case the error for the above pair of wavelengths is as small as 2.9%. As our calculations have shown, this effect is observed only at large solar zenith angles and is due to mutual compensation for changes in the terms $\ln[IS^{1,2}]$ and $-\Delta\tau_a$ in Eq. (4) attendant to changes of τ_a , that is, as τ_a changes, the term $\ln[IS^{1,2}] - \Delta\tau_a$ in Eq. (4) varies only slightly at large θ .

The effect of the solar zenith angle is demonstrated in Table IV, where the errors calculated for model changes of θ from 70 to 89° are presented. The model was constructed for the pair 439.5 and 441.7 nm. The values of the optical depths of the main atmospheric components are also presented in the table. It can be seen that the error due to aerosol drops by more than an order of magnitude in contrast to, for example, δX_{O_3} which even increases with the increase of the zenith angle. The same effect, albeit less pronounced, is also observed for molecular scattering.

Thus, based on these results, the conclusion can be drawn that the effect of the neglect of aerosol contribution to the error in the NO₂ TC reconstruction from measurements in the zenith at large θ is much less pronounced than for measurements against the sun. The physical essence of this effect is connected with the fact that at small solar elevation angles the radiation transmitted through the lower slant atmospheric layers is too weak due to aerosol and molecular scattering. Therefore, the main contribution to the signal comes from the radiation transmitted through sufficiently high slant layers, where the NO₂ content is maximum, as a rule, and the optical depth of aerosol and molecular scattering is much smaller than that of the ground atmospheric layers. As to the contribution of ozone to the error in the NO₂ TC reconstruction, it on the contrary grows with the increase of the solar zenith angle, because the O₃ content is usually maximum at the same altitudes as the NO₂ content. In this connection, it can be assumed that the dense aerosol formations in the troposphere (for example, produced due to volcanic eruption) may have noticeably stronger effect on the error in the NO₂ content determination than that revealed by our estimates obtained for the near-ground aerosol model.

It should be noted in conclusion that the above effect is used in the method of twilight sky

spectroscopy,⁹ and this is why this method is rather sensitive for determination of the NO₂ total content in the stratosphere and low sensitive to the NO₂ content in the troposphere.¹⁸ This method implements the possible way of decreasing one of the main errors in the NO₂ TC reconstruction connected with the uncertainty in the solar constant.⁹ To exclude the Fraunhofer lines from the spectrum of twilight sky, it was normalized to the spectrum of daytime sky. The resultant spectrum (usually within 437–448 nm) had a structure typical of the NO₂ absorption spectrum.

Along with the errors presented in Tables I–III, we have estimated the errors in determination of the total content of the gases under study caused by the deviation of the model profile given by Eq. (4) or (5) from the true one. In so doing we used two different profiles of ozone and nitrogen dioxide: the U.S.A. average-annual model³⁷ and the IAO model³⁶ (for the mid-latitudes in summer). For ozone the difference between the reconstructed values of the total content was within 1%. As to NO₂, it was, on average, 20–25%. This is likely connected with the fact that in the IAO model³⁶ the NO₂ content is maximum in the lower troposphere ($h \sim 0$ km), whereas in the U.S.A. model³⁷ it lies at an altitude of ~ 25 km.

TABLE III. Results of calculation of errors in the NO₂ TOC reconstruction by the two-wavelength method corresponding to Fig. 5. Gas under study is NO₂, $\theta = 89^\circ$, $X_{\text{NO}_2} = 4.6 \cdot 10^{-4}$ atm-cm, $X_{\text{O}_3} = 0.330$ atm-cm, $\lambda_1 = 438.3$ nm (in 0.1-nm step), and $\lambda_2 = 441.7$ nm (in zero step).

$\lambda_1 - \lambda_2$, nm	δu_Σ	δk_g	$\delta J^{1.2}$	$\delta S^{1.2}$	$\delta \theta$	$\delta \tau_m$	$\delta \tau_a$	$\delta \lambda$	$\delta \tau_{\text{O}_3}$
		3%	1%	1%	20'	5%	200%	0.05 nm	50%
		δX_{k_g}	$\delta X_{J^{1.2}}$	$\delta X_{S^{1.2}}$	$\delta X_\theta, \%$	δX_{τ_m}	δX_{τ_a}	δu_λ	δX_{O_3}
438.3–441.7	99.80	24.97	61.44	61.44	10.55	1.71	3.50	36.58	17.92
438.4–441.7	117.09	18.08	66.02	66.02	6.57	2.87	5.21	59.34	32.63
438.5–441.7	168.19	14.17	76.26	76.26	1.97	3.76	5.60	119.23	46.82
438.6–441.7	138.85	11.61	54.83	54.83	5.11	2.28	2.32	109.93	31.80
438.7–441.7	96.10	9.83	46.97	46.97	5.56	1.68	0.53	62.82	27.32
438.8–441.7	83.18	8.83	48.97	48.97	3.92	1.56	0.84	33.78	29.74
438.9–441.7	78.49	8.28	47.64	47.64	3.62	1.30	1.89	26.59	28.79
439.0–441.7	134.90	7.88	81.89	81.89	7.38	2.09	5.55	40.07	54.73
439.1–441.7	207.33	7.61	125.47	125.47	21.43	2.74	11.40	58.90	85.87
439.2–441.7	149.30	7.47	82.32	82.32	8.26	1.42	8.27	75.93	52.72
439.3–441.7	81.34	7.49	46.86	46.86	3.14	0.62	4.55	38.57	25.50
439.4–441.7	59.08	7.71	36.58	36.58	6.81	0.42	3.17	20.17	17.09
439.5–441.7	55.56	7.88	34.52	34.52	7.83	0.34	2.89	19.02	14.50
439.6–441.7	67.10	8.04	39.74	39.74	6.87	0.35	3.51	30.99	16.11
439.7–441.7	102.38	8.36	53.85	53.85	3.89	0.51	4.77	63.76	22.56
439.8–441.7	102.91	8.75	45.28	45.28	6.64	0.40	3.43	77.89	16.98
439.9–441.7	87.09	9.27	39.42	39.42	8.65	0.34	2.42	64.36	12.97
440.0–441.7	114.74	10.00	44.15	44.15	8.41	0.41	2.28	94.32	13.96
440.1–441.7	93.08	10.84	44.96	44.96	9.02	0.42	1.83	65.19	13.01
440.2–441.7	87.64	12.01	48.48	48.48	9.29	0.48	1.45	50.78	12.98
440.3–441.7	71.40	13.57	45.06	45.06	10.77	0.41	0.78	25.30	9.85
440.4–441.7	77.28	15.69	45.42	45.42	11.66	0.37	0.35	37.41	8.00
440.5–441.7	90.62	19.06	49.98	49.98	12.26	0.37	0.03	51.54	6.82
440.6–441.7	109.15	22.68	54.12	54.12	12.81	0.32	0.12	73.13	5.45
$\sigma(\%)$:	76.40 (39.10)	12.10 (4.45)	17.65	47.90 (17.65)	8.10	1.06	3.02	50.40 (18.56)	21.53

TABLE IV. Errors in the NO₂ reconstruction calculated for model changes of the solar zenith angle θ from 70 to 89°. The model was constructed for $\lambda_1 = 439.5$ nm and $\lambda_2 = 441.7$ nm. Gas under study is NO₂, $X_{\text{NO}_2} = 4.6 \cdot 10^{-4}$ atm-cm, $X_{\text{O}_3} = 0.330$ atm-cm, $\lambda_1 = 489.5$ nm ($\tau_{\text{NO}_2} = 0.0080$, $\tau_m = 0.2532$, $\tau_{\pm} = 0.2956$, and $\tau_{\text{O}_3} = 0.00096$), $\lambda_2 = 441.7$ nm ($\tau_{\text{NO}_2} = 0.0045$, $\tau_m = 0.2480$, $\tau_{\pm} = 0.2944$, and $\tau_{\text{O}_3} = 0.00133$) ($\Delta\tau_{\text{NO}_2} = 0.0035$, $\Delta\tau_m = 0.0052$, $\Delta\tau_{\pm} = 0.0012$, and $\Delta\tau_{\text{O}_3} = 0.00037$).

θ°	δu_Σ	δk_g	$\delta J^{1,2}$	$\delta S^{1,2}$	$\delta\theta$	$\delta\tau_m$	$\delta\tau_a$	$\delta\lambda$	$\delta\tau_{\text{O}_3}$
		3%	1%	1%	20'	5%	200%	0.05 nm	50%
		δX_{kg}	$\delta X_{J^{1,2}}$	$\delta X_{S^{1,2}}$	δX_θ	δX_{τ_m}	δX_{τ_a}	δu_λ	δX_{O_3}
70.0	232.5	7.9	142.1	142.1	1.3	3.2	86.1	78.3	7.3
71.0	226.6	7.9	139.1	139.1	1.4	3.3	81.6	76.6	7.4
72.0	218.7	7.9	134.9	134.9	1.4	3.3	76.2	74.3	7.6
73.0	210.7	7.9	130.6	130.6	1.5	3.3	70.7	71.9	7.7
74.0	202.5	7.9	126.2	126.2	1.6	3.4	65.0	69.5	7.9
75.0	194.4	7.9	121.7	121.7	1.8	3.4	59.4	67.0	8.1
76.0	186.1	7.9	117.1	117.1	1.9	3.4	53.9	64.5	8.2
77.0	177.8	7.9	112.5	112.5	2.0	3.4	48.4	61.9	8.5
78.0	169.6	7.9	107.7	107.7	2.1	3.4	43.4	59.3	8.7
79.0	161.1	7.9	102.8	102.8	2.2	3.4	37.9	56.6	9.0
80.0	152.6	7.9	97.9	97.9	2.4	3.3	32.6	53.9	9.3
81.0	144.0	7.9	92.7	92.7	2.5	3.3	27.6	51.0	9.6
82.0	135.2	7.9	87.4	87.4	2.7	3.2	22.7	48.1	10.1
83.0	126.3	7.9	81.9	81.9	2.9	3.0	18.2	45.1	10.6
84.0	117.1	7.9	76.1	76.1	3.1	2.8	13.8	41.9	11.2
85.0	107.7	7.9	70.0	70.0	3.1	2.5	9.8	38.5	11.9
86.0	97.7	7.9	63.4	63.4	3.2	2.1	6.2	34.9	12.9
87.0	87.0	7.9	56.3	56.3	3.3	1.6	2.8	31.0	14.0
88.0	75.1	7.9	48.1	48.1	3.6	1.0	0.5	26.5	15.5
89.0	61.0	7.9	38.0	38.0	6.9	0.4	3.3	20.9	16.5

CONCLUSION

Possible random and systematic errors in the O₃ and NO₂ total content reconstruction have been thoroughly accounted in this paper for two algorithms (two- and four-wavelength ones) with scanning over the spectrum of wavelengths used for data processing. Thus obtained values of the rms errors in the TC determination (5–7% for ozone and 40–76% for nitrogen dioxide) and the prospects for their further decrease support the fruitfulness of the idea⁴ of constructing the ozone nomograms on the basis of calculation for the model of single scattering of light in the atmosphere.

ACKNOWLEDGEMENTS

The authors would like to express their gratitude to S.V. Smirnov for kindly provided results of the total ozone content measurements with the M-124 ozonometer and to S.M. Sakerin for fruitful discussion and valuable remarks at the stage of preparation of this paper.

The work was partially supported by the Russian Foundation for Fundamental Research Grant No. 94-01-01328.

REFERENCES

1. G.P. Gushchin, *Investigation into Atmospheric Ozone* (Gidrometeoizdat, Leningrad, 1963), 269 pp.
2. G.I. Kuznetsov, *Izv. Akad. Nauk SSSR, Fiz. Atmos. Okeana* **11**, No. 6, 647–651 (1975).
3. G.P. Gushchin, K.I. Romashkina, and A.M. Shalamyanskii, *Tr. Gl. Geofiz. Obs.*, No. 357, 106–120 (1976).
4. A.M. Shalamyanskii, *Tr. Gl. Geofiz. Obs.*, No. 357, 205–213 (1976).
5. G.P. Gushchin, *Tr. Gl. Geofiz. Obs.*, No. 406, 63–74 (1978).
6. L.G. Bol'shakova, *Izv. Akad. Nauk SSSR, Fiz. Atmos. Okeana* **12**, No. 9, 969–978 (1976).
7. G.I. Kuznetsov and K.S. Nigmatullina, *Izv. Akad. Nauk SSSR, Fiz. Atmos. Okeana* **13**, No. 8, 896–899 (1977).
8. L.M. Garrison, D.D. Doda, and A.E.S. Green, *Appl. Opt.* **18**, No. 6, 850–855 (1979).
9. J.F. Noxon, E.C. Whipple, Jr., and R.S. Hyde, *J. Geophys. Res.* **84**, No. C8, 5047–5065 (1979).
10. S.P. Perov and A.Kh. Khrgian, *Modern Problems of Atmospheric Ozone* (Gidrometeoizdat, Leningrad, 1980), 288 pp.

11. A.Kh. Khrgian and G.N. Kuznetsov, *Problem of Observation and Study of Atmospheric Ozone* (Moscow State University Press, Moscow, 1981), 216 pp.
12. G.P. Gushchin, *Methodical Instructions for Carrying out and Processing of Observations over the Total Content of Atmospheric Ozone* (Gidrometeoizdat, Leningrad, 1981), 46 pp.
13. G.P. Gushchin and N.N. Vinogradova, *Total Ozone in the Atmosphere* (Gidrometeoizdat, Leningrad, 1983), 240 pp.
14. A.M. Shalamyanskii and K.I. Romashkina, Tr. Gl. Geofiz. Obs., No. 445, 116–123 (1980).
15. G.P. Gushchin, G.V. Kornitskaya, and T.A. Pavlyuchenkova, Tr. Gl. Geofiz. Obs., No. 472, 24–30 (1984).
16. G.P. Gushchin and S.A. Sokolenko, Tr. Gl. Geofiz. Obs., No. 472, 31–35 (1984).
17. K.I. Romashkina, Tr. Gl. Geofiz. Obs., No. 472, 100–107 (1984).
18. I.M. Nazarov, A.N. Nikolaev, and Sh.D. Fridman, *Principles of Remote Methods for Monitoring of Environmental Pollution* (Gidrometeoizdat, Leningrad, 1983), 280 pp.
19. G.P. Gushchin, Meteorol. Gidrol., No. 4, 53 (1984).
20. G.P. Gushchin, in: *Atmospheric Ozone. Proceedings of the Sixth All-Union Symposium* (Gidrometeoizdat, Leningrad, 1987), p. 22.
21. A.M. Lyudchik, A.N. Krasovskii, L.N. Turyshev, and A.F. Chernyavskii, Izv. Akad. Nauk SSSR, Fiz. Atmos. Okeana **24**, No. 1, 75–81 (1988).
22. G.P. Gushchin, S.A. Sokolenko, and M.P. Zhukova, Tr. Gl. Geofiz. Obs., No. 519, 64–73 (1988).
23. A.M. Lyudchik, V.V. Zhuchkevich, A.N. Krasovskii, and L.N. Turyshev, Izv. Akad. Nauk SSSR, Fiz. Atmos. Okeana **25**, No. 1, 45–52 (1989).
24. G. Giovanelli, P. Bonasoni, F. Evangelisti, and T. Georgiadis, SIF Conference Proceedings **20**, 197–213 (1989).
25. A.N. Krasovskii, A.M. Lyudchik, L.Ch. Neverovich, et al., Atm. Opt. **2**, No. 4, 344–349 (1989).
26. A.N. Krasovskii, A.M. Lyudchik, L.Ch. Neverovich, and L.N. Turyshev, Zh. Prikl. Spektrosk. **55**, No. 3, 472–477 (1991).
27. A.S. Elovkhov and A.N. Gruzdev, Atm. Opt. **4**, No. 9, 704–706 (1991).
28. S.D. Ashkinadze, A.A. Balin, S.V. Dolgii, et al., Atmos. Oceanic Opt. **5**, No. 1, 64–67 (1992).
29. A.N. Krasovskii, A.M. Lyudchik, L.Ch. Neverovich, et al., Atmos. Oceanic Opt. **5**, No. 5, 329–331 (1992).
30. V.N. Marichev, Atmos. Oceanic Opt. **8**, No. 8, 615–617 (1995).
31. V.V. Sobolev, *Light Scattering in the Atmospheres of Planets* (Nauka, Moscow, 1972), 350 pp.
32. I.I. Ippolitov, V.S. Komarov, and A.A. Mitsel', in: *Spectroscopic Methods of Atmospheric Sensing* (Nauka, Novosibirsk, 1972), pp 4–44.
33. G.M. Krekov and R.F. Rakhimov, *Optical Model of the Atmospheric Aerosol* (Tomsk Affiliate of the Siberian Branch of the USSR Academy of Sciences, Tomsk, 1986), 294 pp.
34. O. Thomsen, P. Bisling, q. Weitkamp, and W. Michaelis, in: *Proc. 15th ILRC*, Tomsk (1990), Vol. 2, pp. 180–183.
35. O. Thomsen, P. Harteck, and R.R. Reeves, J. Geophys. Res. **68**, No. 24, 6431–6436 (1963).
36. V.E. Zuev and V.S. Komarov, *Statistical Models of the Temperature and Gaseous Constituents of the Atmosphere* (D. Reidel Publishing Company, Dordrecht/Boston/Lancaster/Tokyo, 1987).
37. G.P. Anderson, S.A. Clongh, F.X. Kueizys, J.H. Chetwynd, and E.P. Shettle, *AFGL Atmospheric Constituent Profiles (0–120 km)*, AFGL-TR-86-0110, Hanscom AFB MA 01731 (1986).
38. L.T. Molina and M.J. Molina, J. Geophys. Res. **91**, No. D13, 14501–14508 (1986).
39. M.P. Thekaekara, Appl. Opt. **13**, No. 3, 518–522 (1974).
40. J.C. Arvesen, R.N. Griffin, and B.D. Pearson, Appl. Opt. **8**, No. 11, 2215–2232 (1969).
41. J. Brion, B. Coquart, D. Daumont, et al., in: *Proc. EUROTRAC Symposium 92* (1992), p. 423.
42. W.D. Komhyr and R.D. Evans, Geophys. Res. Lett. **7**, No. 2, 157–160 (1980).
43. J. Skvairs, *Applied Physics* [Russian translation] (Mir, Moscow, 1971), 248 pp.
44. S.G. Rabinovich, *Measurement Error* (Energiya, Leningrad, 1978), 262 pp.
45. A.N. Zaidel', *Errors in Measuring Physical Parameters* (Nauka, Leningrad, 1985), 112 pp.
46. Kh. Shenk, *Theory of Engineering Experiment* [Russian translation] (Mir, Moscow, 1972), 381 pp.
47. G.P. Gushchin and T.A. Pavlyuchenkova, Tr. Gl. Geofiz. Obs., No. 533, 62–66 (1991).
48. G.P. Gushchin and T.A. Pavlyuchenkova, Tr. Gl. Geofiz. Obs., No. 533, 153–157 (1991).
49. V.S. Komarov, S.A. Mikhailov, and D.N. Romashov, *Statistical Structure of the Vertical Distribution of Atmospheric Ozone* (Nauka, Novosibirsk, 1988), 78 pp.